

# The evolution of the martian elastic lithosphere and implications for crustal and mantle rheology

M. Grott\*, D. Breuer

*Institute of Planetary Research, German Aerospace Center (DLR), Rutherfordstraße 2, 12489 Berlin, Germany*

Received 30 May 2007; revised 15 August 2007

Available online 12 September 2007

## Abstract

Estimates of the martian elastic lithosphere thickness  $T_e$  imply that  $T_e$  increased from around 20 km in the Noachian to about 70 km in the Amazonian period. A phase of rapid lithospheric growth is observed during the Hesperian and we propose that this elastic thickness history is a consequence of the martian crustal rheology and its thermal evolution. A wet crustal rheology is found to generate a mechanically incompetent layer in the lower crust during the early evolution and the rapid growth of  $T_e$  during the Hesperian results from the disappearance of this layer due to planetary cooling. The incompetent layer and the related rapid lithospheric growth are absent for a dry basaltic crustal rheology, which is therefore incompatible with the observations. Furthermore, we find that the observed elastic thickness evolution is best compatible with a wet mantle rheology, although a dry mantle cannot be ruled out. It therefore seems likely that rheologically significant amounts of water were retained in the Martian crust and mantle after planetary accretion.

© 2007 Elsevier Inc. All rights reserved.

*Keywords:* Mars; Mars, interior; Thermal histories; Geophysics

## 1. Introduction

Planetary lithospheres exhibit nonzero mechanical strength over geological timescales and their flexural rigidity is generally expressed in terms of the elastic lithosphere thickness  $T_e$ . On the Earth, the continental and oceanic lithosphere have had distinct physical and chemical evolutions and their respective effective elastic thickness is controlled by different processes. The oceanic lithosphere is relatively young, has a single-layer rheology and  $T_e$  largely depends on the local thermal age (Watts, 1978). It roughly follows the depth to the 450–600 °C isotherm, reflecting the growth of mechanical strength as the lithosphere cools (Watts, 1978; Watts et al., 1980; Caldwell and Turcotte, 1979; McNutt and Menard, 1982).

In contrast, this simple dependence of  $T_e$  on temperature is not applicable to the continents. Although there is a relation between lithospheric strength and thermal state (Karner et al., 1983; Sahagian and Holland, 1993),  $T_e$  in the conti-

nents cannot be described by a relationship with only one parameter (Cochran, 1980; McNutt et al., 1988; McNutt, 1990; Watts, 1992; Kruse and Royden, 1994; Watts and Burov, 2003). In addition to the geotherm,  $T_e$  depends on the state of the crust–mantle interface (mechanical coupling or decoupling of crust and mantle), the thicknesses and proportions of the mechanically competent layers and intraplate stresses (Burov and Diament, 1995).

As a consequence,  $T_e$  estimates on the continents vary over a wide range although they are not randomly distributed. Rather, a bimodal distribution with a primary peak at 10–30 km and a secondary peak around 70–90 km is observed (Watts, 1992). This bimodal structure is the consequence of a change of the mechanical state of the crust–mantle interface, with low  $T_e$  corresponding to mechanical decoupling and high  $T_e$  corresponding to mechanical coupling of crust and mantle. Decoupling in the young and warm lithosphere is caused by the presence of an incompetent layer in the lower crust which later disappears due to lithospheric cooling. This bimodal distribution of elastic thickness values is not observed for the oceans and is a direct consequence of the multilayer rheology of the continental lithosphere (Burov and Diament, 1995).

\* Corresponding author.

E-mail address: [matthias.grott@dlr.de](mailto:matthias.grott@dlr.de) (M. Grott).

Estimates of the martian elastic lithosphere thickness imply that  $T_e$  evolved from values around 20 km in the Noachian (McGovern et al., 2004; Grott et al., 2005, 2007; Kronberg et al., 2007) to around 70 km in the Amazonian period (McGovern et al., 2004; Belleguic et al., 2005) and this general trend is well understood in terms of planetary cooling as predicted by thermal evolution models (Hauck and Phillips, 2002; Schumacher and Breuer, 2006). However, the data also implies that the lithospheric thickness rapidly increased during the Hesperian period (McGovern et al., 2004), which may not be explained by the depth evolution of a single isotherm and is reminiscent of the bimodal  $T_e$  distribution on Earth's continents.

Therefore, Schumacher and Breuer (2006) have studied the depth evolution of the isotherms corresponding to the onset of plasticity in diabase rock and olivine, i.e., the temperatures above which mechanical strength is lost in the crust and mantle, respectively. They argue that during the early evolution lithospheric strength is carried by the crust alone and that only after the upper mantle has sufficiently cooled  $T_e$  is controlled by the brittle–ductile transition in olivine.

In this paper we compile  $T_e$  estimates to reconstruct the martian elastic thickness history. This data is compared to models of the elastic thickness evolution, which we construct using thermal evolution models. The elastic thicknesses are calculated using the strength envelope formalism and the mechanical state of the crust–mantle interface is taken into account (Burov and Diament, 1995). Furthermore, the influence of crustal and mantle rheology on the evolution of the martian elastic lithosphere thickness will be investigated.

## 2. Data

The elastic thickness of Earth's continents has been estimated in numerous studies and Fig. 1a shows a compilation by Watts (2001) of  $T_e$  values as a function of plate age (see his Table 6.2 and references therein). Although the data exhibits a large scatter a clear correlation of  $T_e$  with plate age is visible. To demonstrate this, we have calculated average  $T_e$  for time-bins of 0–500, 250–750, 500–1000, 750–2000 and 1000–3000 Myr, and the results are indicated by shaded rectangles in Fig. 1a. During the first 1000 Myr,  $T_e$  slowly grows from  $23 \pm 18$  to  $25 \pm 20$  and  $37 \pm 16$  km before rapidly increasing to  $56 \pm 27$  and  $64 \pm 32$  km between 750–2000 and 1000–3000 Myr, respectively. Therefore,  $T_e$  values exhibit a bimodal distribution with low  $T_e$  corresponding to young and high  $T_e$  corresponding to old lithospheric plates.

Mostly owing to the limited resolution of the available gravity data, estimates of the elastic lithosphere thickness are much sparser for Mars. Furthermore, the determination of plate and loading ages pose severe problems, and the time of loading can usually only be constrained to within a specific epoch, which might span several gigayears. We have compiled  $T_e$  estimates derived from gravity and topography data (McGovern et al., 2004; Belleguic et al., 2005), forward modeling of thrust faults (Schultz and Watters, 2001; Grott et al., 2007) and the analysis of rift flank uplift (Grott et al., 2005; Kronberg et al., 2007) and converted the epoch of the loading event to absolute ages using

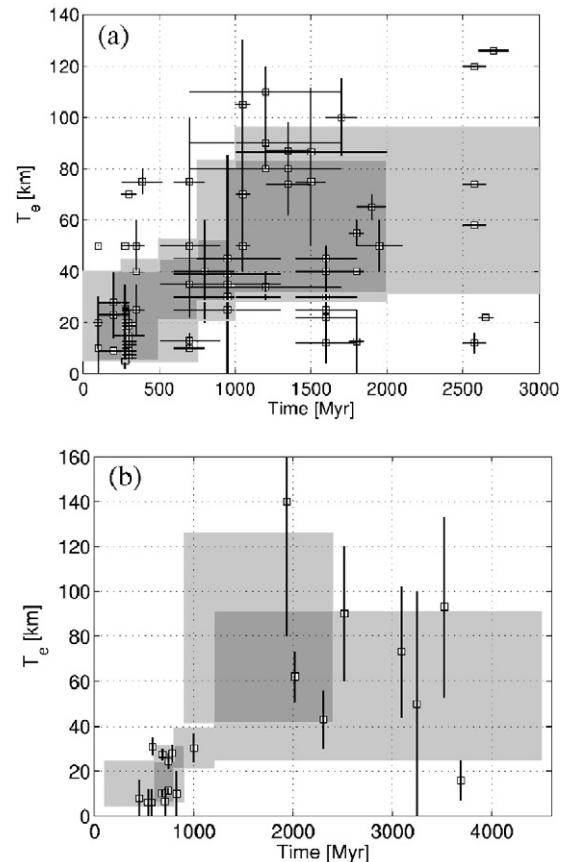


Fig. 1. (a) Elastic thickness estimates for Earth's continents as a function of plate age. [Data adopted from the compilation of Watts (2001), see his Table 6.2 and references therein.] Average elastic thickness values have been computed for the time-bins 0–500, 250–750, 500–1000, 750–2000 and 1000–3000 Myr, yielding average  $T_e$  of  $23 \pm 18$ ,  $25 \pm 20$ ,  $37 \pm 16$ ,  $56 \pm 27$  and  $64 \pm 32$  km, respectively. The average elastic thickness values for each time-bin are indicated by shaded rectangles and overlapping bins have stronger shading. (b) Elastic thickness estimates for Mars as a function of time. Average elastic thickness values have been computed for time-bins corresponding to the Noachian (100–800 Myr), Noachian–Hesperian (600–900 Myr), Hesperian (800–1200 Myr), Hesperian–Amazonian (900–2400 Myr) and Amazonian (1200–4500 Myr) epochs, yielding average  $T_e$  of  $15 \pm 10$ ,  $19 \pm 13$ ,  $30 \pm 7$ ,  $84 \pm 42$  and  $58 \pm 33$  km, respectively. The average elastic thickness for each time-period is indicated by shaded rectangles and overlapping bins have stronger shading.

the cratering chronological model of Hartmann and Neukum (2001). We do not consider estimates for which only lower limits on  $T_e$  are available and have substituted 0 km for a lower limit if only upper bounds existed. Also, we have calculated the mean and standard error for each structure where multiple estimates were available.

The resulting elastic thickness estimates comprise 20 data-points which are shown as a function time in Fig. 1b. Averages of  $T_e$  for the martian epochs have been calculated by merging the data into time-bins corresponding to the Noachian (100–800 Myr), Noachian–Hesperian (600–900 Myr), Hesperian (800–1200 Myr), Hesperian–Amazonian (900–2400 Myr) and Amazonian (1200–4500 Myr) periods. The time coordinate of individual data-point has been shifted from the center of the corresponding epochs for better visibility. Mean elastic thicknesses

Table 1  
Mean elastic thickness in the martian epochs

Epoch	Time [Myr]	$T_e$ [km]
Noachian	100–800	$15 \pm 10$
Noachian–Hesperian	600–900	$19 \pm 13$
Hesperian	800–1200	$30 \pm 7$
Hesperian–Amazonian	900–2400	$84 \pm 42$
Amazonian	1200–4500	$58 \pm 33$

as well as the spread of the data have thus been calculated and are indicated by shaded rectangles in Fig. 1b.

During the Noachian to Hesperian periods, observed elastic thickness values range from  $\sim 10$  km at rifts (Grott et al., 2005; Kronberg et al., 2007) to about 30 km at lobate scarps (Schultz and Watters, 2001; Grott et al., 2007). Average  $T_e$  ranges from  $15 \pm 10$  to  $19 \pm 13$  and  $30 \pm 7$  km during the Noachian, Noachian–Hesperian and Hesperian periods. During the Hesperian–Amazonian and Amazonian periods,  $T_e$  rapidly increases to  $84 \pm 42$  and  $58 \pm 33$  km, revealing a rapidly growing elastic thickness during the Hesperian, with young plates showing small  $T_e$  around 20 km and old plates showing large  $T_e$  around 70 km. These results are summarized in Table 1.

### 3. Modeling

#### 3.1. Thermal evolution

The thermal evolution of Mars is modeled by solving the energy balance equations for the core, mantle and lithosphere, treating the mantle energy transport by parametrized convection models using scaling laws for stagnant lid convection (Grasset and Parmentier, 1998). The model is similar to that of Schumacher and Breuer (2006) but we ignore partial melting and crustal production. Instead, we assume that the bulk of the crust is primordial and although there is evidence for late crustal production even after 4 Gyr (Hartmann et al., 1999; Hartmann and Berman, 2000; Neukum et al., 2004; Grott, 2005), its volumetric contribution is probably minor on a global scale (Nimmo and Tanaka, 2005). A sketch of the model setup is shown in Fig. 2 where a typical temperature profile is shown as a function of depth. Temperatures are assumed to increase adiabatically in the core and mantle and linearly in the thermal boundary layers.

Energy balance equations for the mantle and the core are given by

$$\rho_m c_m V_m \epsilon_m \frac{dT_m}{dt} = -q_m A_m + q_c A_c + Q_m V_m \quad (1)$$

and

$$\rho_c c_c V_c \epsilon_c \frac{dT_c}{dt} = -q_c A_c, \quad (2)$$

where  $\rho_m$  and  $\rho_c$  are the density,  $c_m$  and  $c_c$  the heat capacity,  $V_m$  and  $V_c$  the volume and  $A_m$  and  $A_c$  the surface areas of mantle and core, respectively.  $T_m$  is the upper mantle temperature, i.e., the temperature at the top of the convecting portion of the mantle and  $T_c$  is the temperature at the core–mantle boundary. The constants  $\epsilon_m$  and  $\epsilon_c$  are the ratios between the average and

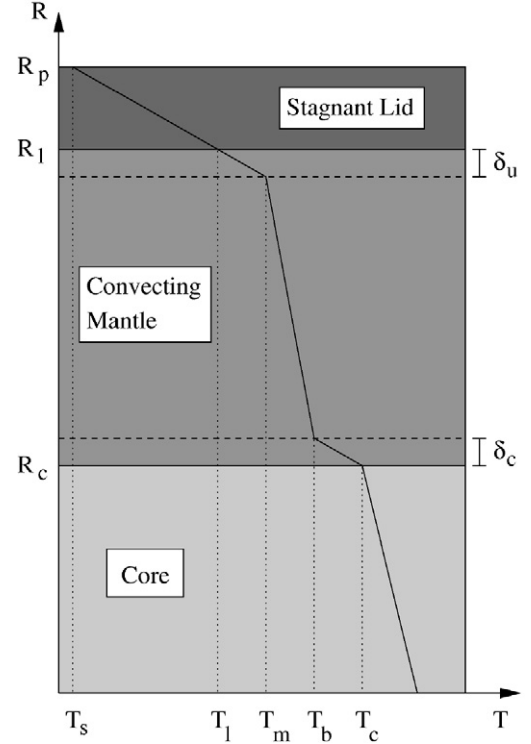


Fig. 2. Sketch of the model setup used for thermal evolution calculations, indicating the temperature profile as a function of radius. Energy balance equations are solved for the core, mantle and stagnant lid using parametrized convection models. The listed quantities are discussed in the text.

upper mantle and core–mantle boundary temperatures, respectively.  $q_m$  is the heat flow from the mantle into the base of the stagnant lid and  $Q_m$  is the mantle energy generation rate.  $q_c$  is the heat flow from the core into the mantle and  $t$  is time. The core cools by conducting heat into the mantle and the mantle is heated from below by the core and by the decay of radiogenic elements. It cools by losing energy to the stagnant lid.

The amount of radiogenic heating in the mantle depends on the bulk concentration of radioactive nuclides and their distribution between the mantle and the crust. At a given time, the mantle volumetric heating rate is given by

$$Q_m(t) = \sum_i Q_i \exp(-\lambda_i t) \left( 1 + \frac{V_{cr}}{V_m} (1 - \Lambda) \right) \quad (3)$$

for  $\Lambda < 1 + (V_m/V_{cr})$ , where  $V_{cr}$  is the crustal volume and  $\Lambda$  the crustal enrichment factor with respect to the primitive mantle. The sum extends over all radioactive species and  $\lambda_i$  and  $Q_i$  are the species half life and heat generation rate, respectively. The crustal volumetric heating rate  $Q_{cr}(t)$  is then calculated from mass balance constraints. For the bulk abundance of radioactive isotopes in the primitive martian mantle we use the model by Treiman et al. (1986) (Table 2) and adopt a crustal enrichment factor of 5 (Breuer and Spohn, 2003).

The heat flow out of the mantle  $q_m$  and the core  $q_c$  are calculated from

$$q_m = k_m \frac{T_m - T_l}{\delta_u} \quad (4)$$

Table 2

Today's radiogenic heat production rates for the models considered, corresponding to 16 ppb U, 64 ppb Th and 160 ppm K (Treiman et al., 1986)

Species	$\lambda$ [yr]	$Q$ [W kg <sup>-1</sup> ]
<sup>238</sup> U	$4.47 \times 10^9$	$1.50 \times 10^{-12}$
<sup>235</sup> U	$7.04 \times 10^8$	$6.46 \times 10^{-14}$
<sup>232</sup> Th	$1.4 \times 10^{10}$	$1.69 \times 10^{-12}$
<sup>40</sup> K	$1.25 \times 10^9$	$5.56 \times 10^{-13}$

and

$$q_c = k_m \frac{T_c - T_b}{\delta_c}, \quad (5)$$

where  $k_m$  is the mantle thermal conductivity,  $T_l$  the temperature at the base of the lithosphere,  $T_b$  the temperature at the base of the mantle and  $\delta_u$  and  $\delta_c$  are the thicknesses of the upper and lower thermal boundary layers, respectively (cf. Fig. 2).  $T_b$  is given by the adiabatic temperature increase in the mantle

$$T_b = T_m + \frac{\alpha g T_m}{c_m} \Delta R, \quad (6)$$

where  $\Delta R = R_l - R_c - \delta_u - \delta_c$  and  $R_c$  and  $R_l$  are the core and the lithospheric radius, respectively. The lithospheric basal temperature  $T_l$  is defined as the temperature at which the viscosity has grown by one order of magnitude with respect to the convecting mantle and is thus a function of mantle temperature and the rate of change of viscosity with temperature (Davaille and Jaupart, 1993; Grasset and Parmentier, 1998; Choblet and Sotin, 2000). It is given by

$$T_l = T_m - 2.21 \frac{RT_m^2}{A}, \quad (7)$$

where  $R$  is the gas constant and  $A$  is the activation energy for viscous deformation.

The thickness of the upper thermal boundary layer is derived from boundary layer theory (Turcotte and Schubert, 2002) and given by

$$\delta_u = (R_l - R_c) \left( \frac{Ra_{\text{crit}}}{Ra} \right)^\beta, \quad (8)$$

where  $Ra_{\text{crit}}$  is the critical Rayleigh number and  $\beta = 1/3$ . The Rayleigh number  $Ra$  is defined by

$$Ra = \frac{\alpha \rho_m g \Delta T (R_l - R_c)^3}{\kappa \eta}, \quad (9)$$

where  $\Delta T = T_m - T_l + T_b - T_c$ ,  $\kappa$  is the mantle thermal diffusivity,  $\alpha$  the thermal expansivity,  $g$  the surface gravitational acceleration and  $\eta$  the mantle viscosity given by

$$\eta = \eta_0 \exp \left( \frac{A (T_{\text{ref}} - T_m)}{R T_{\text{ref}} T_m} \right). \quad (10)$$

Here,  $\eta_0$  is the reference viscosity at the temperature  $T_{\text{ref}} = 1600$  K. The thickness of the lower thermal boundary layer is given by

$$\delta_c = \left( \frac{\kappa \eta_c Ra_{\text{crit}}}{\alpha \rho_m g_c (T_c - T_b)} \right)^{\frac{1}{3}}, \quad (11)$$

where  $g_c$  is the gravitational acceleration at the core–mantle boundary and  $\eta_c$  the viscosity at temperature  $(T_c + T_m)/2$  (Richter, 1978).

The stagnant lid thickness  $D_l$  is determined by the energy balance at the lithospheric base (Schubert et al., 1979; Spohn and Schubert, 1982; Schubert and Spohn, 1990; Spohn, 1991). Neglecting volcanic heat transfer, the stagnant lid thickness  $D_l$  is determined by

$$\rho_m c_m (T_m - T_l) \frac{D_l}{dt} = -q_m - k_m \frac{\partial T}{\partial r} \Big|_{r=R_l}, \quad (12)$$

where  $\partial T / \partial r|_{r=R_l}$  is the thermal gradient at the base of the lithosphere. The rate of lithospheric growth therefore depends on the difference between the heat  $q_m$  transferred into the lithospheric base and the amount of heat  $k_m \partial T / \partial r|_{r=R_l}$  conducted away towards the surface.

The thermal gradient at the lithospheric base is calculated by solving the heat conduction equation for the lithosphere

$$\frac{1}{r^2} \frac{\partial}{\partial r} \left( r^2 k_l \frac{\partial T}{\partial r} \right) + Q_l = 0, \quad (13)$$

where  $k_l$  and  $Q_l$  are the lithospheric thermal conductivity and heat production rate, respectively. Together with the temperatures  $T_s$  and  $T_l$  at the surface and the base of the lithosphere, Eq. (13) poses a boundary value problem which is solved using a shooting method. Once the temperatures in the lithosphere have been determined,  $\partial T / \partial r|_{r=R_l}$  may be evaluated. This approach allows for the introduction of layers with different properties as  $k_l$  and  $Q_l$  may be depth dependent. To include the influence of a thermally isolating crust that is enriched in radioactive elements, we prescribe  $k_l = k_{\text{cr}}$  and  $Q_l = Q_{\text{cr}}$  at depths shallower than  $R_{\text{cr}} = R_p - D_{\text{cr}}$ , where  $D_{\text{cr}}$  and  $k_{\text{cr}}$  are the crustal thickness and thermal conductivity, respectively.

### 3.2. Elastic thickness

Given the thermal structure of the martian lithosphere, elastic thicknesses are calculated using the strength envelope formalism (McNutt et al., 1988) for the two-layer system consisting of crust and mantle. The strength envelope is a measure for the amount of stress the lithosphere can sustain before yielding and is given by the lower of the two stresses necessary to induce frictional sliding  $\sigma_B$  and ductile creep  $\sigma_D$ . Frictional sliding or brittle deformation is largely independent of rock type (Byerlee, 1978) and initiates as soon as extensional stresses exceed

$$\sigma_B = \begin{cases} 0.786 \sigma_v, & \sigma_v \leq 529.9 \text{ MPa}, \\ 56.7 \text{ MPa} + 0.679 \sigma_v, & \sigma_v > 529.9 \text{ MPa}, \end{cases} \quad (14)$$

where  $\sigma_v$  is the lithostatic pressure (Mueller and Phillips, 1995). In compression, failure occurs for

$$\sigma_B = \begin{cases} -3.68 \sigma_v, & \sigma_v \leq 113.2 \text{ MPa}, \\ -176.6 \text{ MPa} - 2.12 \sigma_v, & \sigma_v > 113.2 \text{ MPa}. \end{cases} \quad (15)$$

The onset of ductile deformation is governed by the flow law

$$\sigma_D = \left( \frac{\dot{\epsilon}}{B} \right)^{\frac{1}{n}} e^{Q/nRT}, \quad (16)$$

Table 3  
Rheological parameters used in this study

Rheology	$B$ [Pa $^{-n}$ s $^{-1}$ ]	$n$	$Q$ [kJ mol $^{-1}$ ]	$T(\sigma_y)$ [K]	Reference
Diabase (dry)	$1.1 \times 10^{-26}$	4.7	488	1029	Mackwell et al. (1998)
Diabase (wet)	$3.1 \times 10^{-20}$	3.05	276	744	Caristan (1982)
Olivine (dry)	$2.4 \times 10^{-16}$	3.5	540	1065	Karato et al. (1986)
Olivine (wet)	$1.9 \times 10^{-15}$	3.0	420	922	Karato et al. (1986)

Table 4  
Parameters used in this study

Variable	Physical meaning	Value	Units
$R_p$	Planetary radius	$3390 \times 10^3$	m
$R_c$	Core radius	$1550 \times 10^3$	m
$g$	Surface gravity	3.7	m s $^{-2}$
$T_s$	Surface temperature	220	K
$\Delta T_{cm}$	Core–mantle temperature difference	300	K
$\rho_{cr}$	Crustal density	2900	kg m $^{-3}$
$\rho_m$	Mantle density	3500	kg m $^{-3}$
$\rho_c$	Core density	7200	kg m $^{-3}$
$c_m$	Mantle heat capacity	1142	J kg $^{-1}$ mol $^{-1}$
$c_c$	Core heat capacity	840	J kg $^{-1}$ mol $^{-1}$
$\epsilon_m$	Ratio of mean and upper mantle temperature	1.0	
$\epsilon_c$	Ratio of mean and upper core temperature	1.1	
$R$	Gas constant	8.3144	J K $^{-1}$ mol $^{-1}$
$T_{ref}$	Reference temperature	1600	K
$k_m$	Mantle thermal conductivity	4	W m $^{-1}$ K $^{-1}$
$\alpha$	Thermal expansion coefficient	$2 \times 10^{-5}$	K $^{-1}$
$\kappa$	Mantle thermal diffusivity	$10^{-6}$	m $^2$ s $^{-1}$
$\Lambda$	Crustal enrichment factor	5	
$Ra_{crit}$	Critical Rayleigh number	450	
$\dot{\epsilon}$	Strain rate	$10^{-17}$	s $^{-1}$

where  $\dot{\epsilon}$  is strain rate and  $B$ ,  $n$  and  $Q$  are rheological parameters. In the absence of information on the active deformation mechanisms we adopt a strain rate of  $10^{-17}$  s $^{-1}$  (e.g., McGovern et al., 2004) and use parameters appropriate for wet (Caristan, 1982) and dry diabase (Mackwell et al., 1998) for the candidate crustal rheologies and wet and dry olivine (Karato et al., 1986) for the candidate mantle rheologies. The different rheological parameters used in this study are summarized in Table 3.

Given the thermal structure of the lithosphere, yield envelopes may be calculated if rheologies for the crust and mantle are prescribed. The elastic thickness of the individual crustal and mantle layers,  $T_{e,c}$  and  $T_{e,m}$ , are calculated assuming zero bending moment, i.e., a non-flexed plate. In this case the mechanical and elastic thicknesses coincide (McNutt, 1984) and  $T_e$  is limited by the depth at which the plate loses its mechanical strength due to ductile flow. Following Burov and Diament (1995), we assume a bounding stress of  $\sigma_y = 15$  MPa.

The elastic thickness of the compound system consisting of the crust and mantle layers then depends on whether the individual layers are welded or separated by a layer of incompetent crust. If the layers are detached,  $T_e$  is given by

$$T_e = (T_{e,m}^3 + T_{e,c}^3)^{\frac{1}{3}}, \quad (17)$$

where  $T_{e,m}$  and  $T_{e,c}$  are the thicknesses of the elastic portions of the mantle and crust, respectively (e.g., Burov and Diament,

1995). If, however,  $T_{e,c}$  equals the crustal thickness and no layer of incompetent crust exists,  $T_e$  is simply given by the sum of the individual components which then act as a single plate and

$$T_e = T_{e,m} + T_{e,c}. \quad (18)$$

Given the bounding stress below which the individual layers lose their mechanical strength, Eq. (16) may be used to determine the temperature associated with ductile failure. It is given by

$$T(\sigma_y) = \frac{Q}{R} \left[ \log \left( \frac{\sigma_y^n B}{\dot{\epsilon}} \right) \right]^{-1} \quad (19)$$

and the temperatures above which the investigated materials lose their mechanical strength are given in Table 3.

### 3.3. Parameters

The parameters used in the calculations are summarized in Table 4 and we have varied the initial upper mantle temperature  $T_m$ , crustal thermal conductivity  $k_{cr}$  and crustal thickness  $D_c$  in the bounds specified below to study the influence of these parameters on the elastic thickness evolution. We have also used different reference viscosities to study the influence of water in the martian mantle and the nominal values of these parameters are summarized in Table 5.

The initial temperature of the martian mantle is largely unknown and estimates which are consistent with the martian

Table 5  
Parameters of the nominal model

Variable	Physical meaning	Value	Units
$T_m$	Initial mantle temperature	1800	K
$\eta_{0,wet}$	Reference viscosity, wet mantle	$10^{19}$	Pa s
$\eta_{0,dry}$	Reference viscosity, dry mantle	$10^{21}$	Pa s
$k_{cr}$	Crustal thermal conductivity	3	$\text{W m}^{-1} \text{K}^{-1}$
$D_c$	Crustal thickness	$50 \times 10^3$	m

chemical evolution and observed crustal thickness (Wieczorek and Zuber, 2004) range from 1700 to 2000 K (Hauck and Phillips, 2002; Schumacher and Breuer, 2006; Parmentier and Zuber, 2007). Initial core temperatures may be constrained from the magnetic field history which requires either an early episode of plate tectonics, a phase of magma ocean overturn or a superheated core (Nimmo and Stevenson, 2000; Breuer and Spohn, 2003; Williams and Nimmo, 2004; Elkins-Tanton et al., 2005). There is only scarce evidence for plate tectonics on early Mars (Connerney et al., 2005) and we do not consider models involving magma ocean overturn, as these result in a stable mantle stratification which suppresses thermal convection (Elkins-Tanton et al., 2003). However, the influence of a stably stratified mantle on the elastic thickness evolution will be briefly discussed in Section 6. We favor a superheated core and assume a temperature difference of 300 K between upper core and mantle temperatures. In this study, initial upper mantle temperatures are varied between 1700 and 1900 K.

The thermal conductivity of the majority of compact volcanic materials ranges from 1.5 to 3.5  $\text{W m}^{-1} \text{K}^{-1}$  at ambient conditions (Clauser and Huenges, 1995) and decreases with temperature (Clauser and Huenges, 1995; Seipold, 1998). In addition to the temperature dependence, the structure of the material can change thermal conductivity significantly. Fractured and porous material has a reduced thermal conductivity and impact gardening may result in the formation of a brecciated upper crust. However, this reduction may be balanced by ice fill in the pores as ice cemented soil has conductivities of 2.5  $\text{W m}^{-1} \text{K}^{-1}$  (Mellon et al., 2004). Also hydrothermal circulation in the upper crust may increase conductivity by a factor of 2 to 3 (Parmentier and Zuber, 2007). Given these unknowns, we vary the thermal conductivity between 2.5 and 3.5  $\text{W m}^{-1} \text{K}^{-1}$ .

The thickness of the martian crust has been constrained from gravity and topography data (Zuber et al., 2000; Neumann et al., 2004; Wieczorek and Zuber, 2004) as well as the absence of large scale viscous topographic relaxation (Nimmo and Stevenson, 2001). Combining the different constraints on  $D_c$ , a globally averaged crustal thickness of  $50 \pm 12$  km (Wieczorek and Zuber, 2004) seems likely and we vary  $D_c$  between 40 and 60 km.

The rheology and thus viscosity of the mantle are a major factor controlling the thermal evolution of a planet. There is evidence that petrologically significant amounts of water are present in the martian mantle (Médard and Grove, 2006) and isotopic evidence suggests that the shergottite parent magmas contained small amounts of water (McSween et al., 2001). Considering that only little water is needed to be rheologically

significant (Mei and Kohlstedt, 2000a, 2000b), the rheology of the martian mantle would be best approximated by a wet olivine rheology. If water were present in the mantle, the viscosity would be expected to be comparable to that of the Earth's mantle and a reference viscosity of  $10^{19}$  Pa s at a temperature of 1600 K would be appropriate (Karato and Wu, 1993). However, it is also possible that Mars did not retain any water during its accretion and water was only added at a later evolutionary stage (Dreibus and Wanke, 1987). In this case, the martian mantle would be dry and a higher reference viscosity of  $10^{21}$  Pa s would be appropriate. So far, no consensus on the abundance of water in the martian mantle has been reached and we will consider both models here.

## 4. Results

### 4.1. Influence of mantle viscosity

The nominal thermal evolution models for a (a) wet and (d) dry mantle rheology are shown in Fig. 3, where contour plots of the temperature as a function of time and depth are given. The isotherms corresponding to the loss of mechanical strength in wet diabase (744 K), dry diabase (1029 K), wet olivine (922 K) and dry olivine (1065 K) are indicated. The base of the crust is marked by a horizontal line and the crust is slightly shaded.

For a wet mantle (Fig. 3a), convection is more vigorous and the thermal boundary layers at the top and bottom of the mantle are very thin. Thus the planet efficiently cools and a lot of heat is transported to the near surface layers, resulting in a thin lithosphere. In contrast to the wet mantle for which the thermal evolution roughly parallels the instantaneous radiogenic heat production, a dry mantle rheology (Fig. 3d) results in thick thermal boundary layers. Heat is stored in the mantle and the near surface layers remain relatively cool (cf. Fig. 3a). The faster cooling of the model with a wet mantle rheology is also evident from the depth development of the isotherms: while the depth to a particular isotherm rapidly increases for the wet mantle, it varies only slowly after a phase of initial cooling for the dry mantle.

Note that the early thermal evolution is strongly influenced by the adopted initial conditions in terms of the initial upper mantle temperature  $T_m$  and the ability of the mantle to transport heat to the lithospheric base. Note also that for the dry mantle temperature differences caused by the initial conditions are preserved during the entire evolution, whereas for the wet mantle solutions with different initial conditions converge at large times.

Snapshots of the strength envelopes corresponding to a wet mantle rheology at different times are shown for a wet crustal rheology in Fig. 3b. The wet mantle results in a hot lithosphere and at 500 and 1500 Myr after core formation the mantle carries no strength at all. Rigidity is located in the wet crust and only after the upper mantle has cooled sufficiently at  $\sim 1600$  Myr, it starts to contribute to the lithospheric strength. At 2500 Myr, the incompetent ductile layer in the lower crust vanishes and the crustal and mantle sublayers become coupled. From there on,

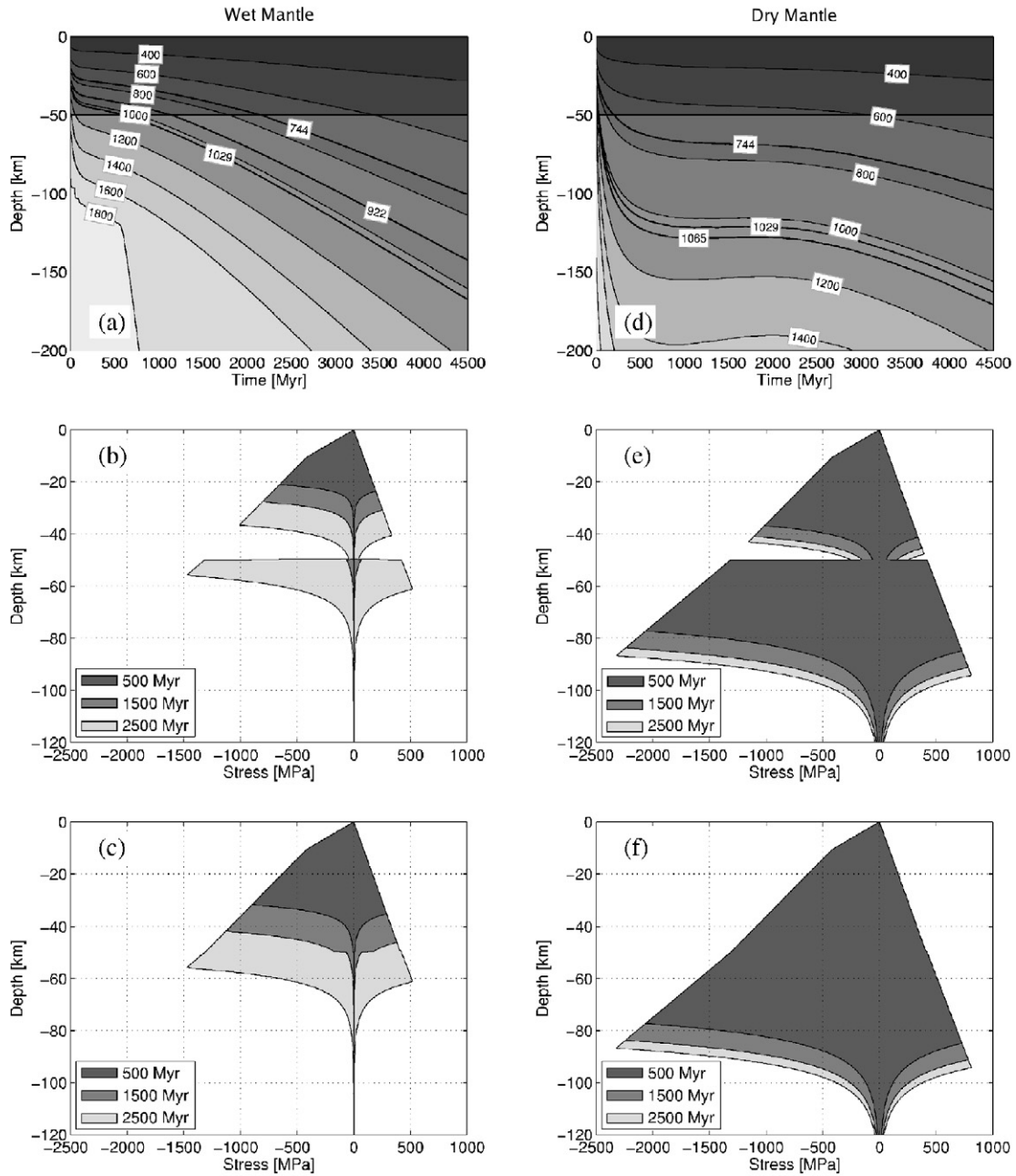


Fig. 3. (a) Contour plot of temperature  $T$  as a function of time and depth for the reference thermal evolution model with a wet mantle rheology and  $\eta_0 = 10^{19}$  Pa s. The isotherms corresponding to the loss of mechanical strength in wet diabase (744 K), dry diabase (1029 K) and wet olivine (922 K) are also indicated. The base of the crust is marked by a horizontal line and the area above is slightly shaded. (b) Yield strength envelopes for the reference thermal evolution model given in (a) and a wet crustal and mantle rheology at different times. (c) Same as (b), but for a dry crustal and wet mantle rheology. (d) Same as (a), but for the reference thermal evolution model with a dry mantle rheology and  $\eta_0 = 10^{21}$  Pa s. The isotherms corresponding to the loss of mechanical strength in wet diabase (744 K), dry diabase (1029 K) and dry olivine (1065 K) are indicated. (e) Yield strength envelopes for the reference thermal evolution model given in (d) and a wet crustal and dry mantle rheology at different times. (f) Same as (e), but for a dry crustal and dry mantle rheology.

crust and mantle act as a single plate and the evolution of the elastic lithosphere thickness is governed by planetary cooling.

If a dry crust is assumed (c), ductile yielding in the wet mantle will set in at lower temperatures than those necessary to initiate flow in the crust (cf. Table 3). Consequently, a rigid mantle layer can only develop after the entire crust has become mechanically strong and no incompetent crustal layer develops. The notch in the strength envelope is missing and lithospheric strength grows continuously.

Strength envelopes corresponding to a dry mantle rheology are also shown for a (e) wet and (f) dry crust in Fig. 3. The dry mantle yields much lower lithospheric temperatures and the overall strength of the lithosphere is increased. An incompetent layer in the lower crust develops for the wet crustal rheology, but coupling already sets in around 500 Myr. If a dry crust is assumed (Fig. 3f), the yield temperatures for crust and mantle are similar (cf. Table 3), there is no notch in the strength envelope and no incompetent crustal layer develops. Rather,

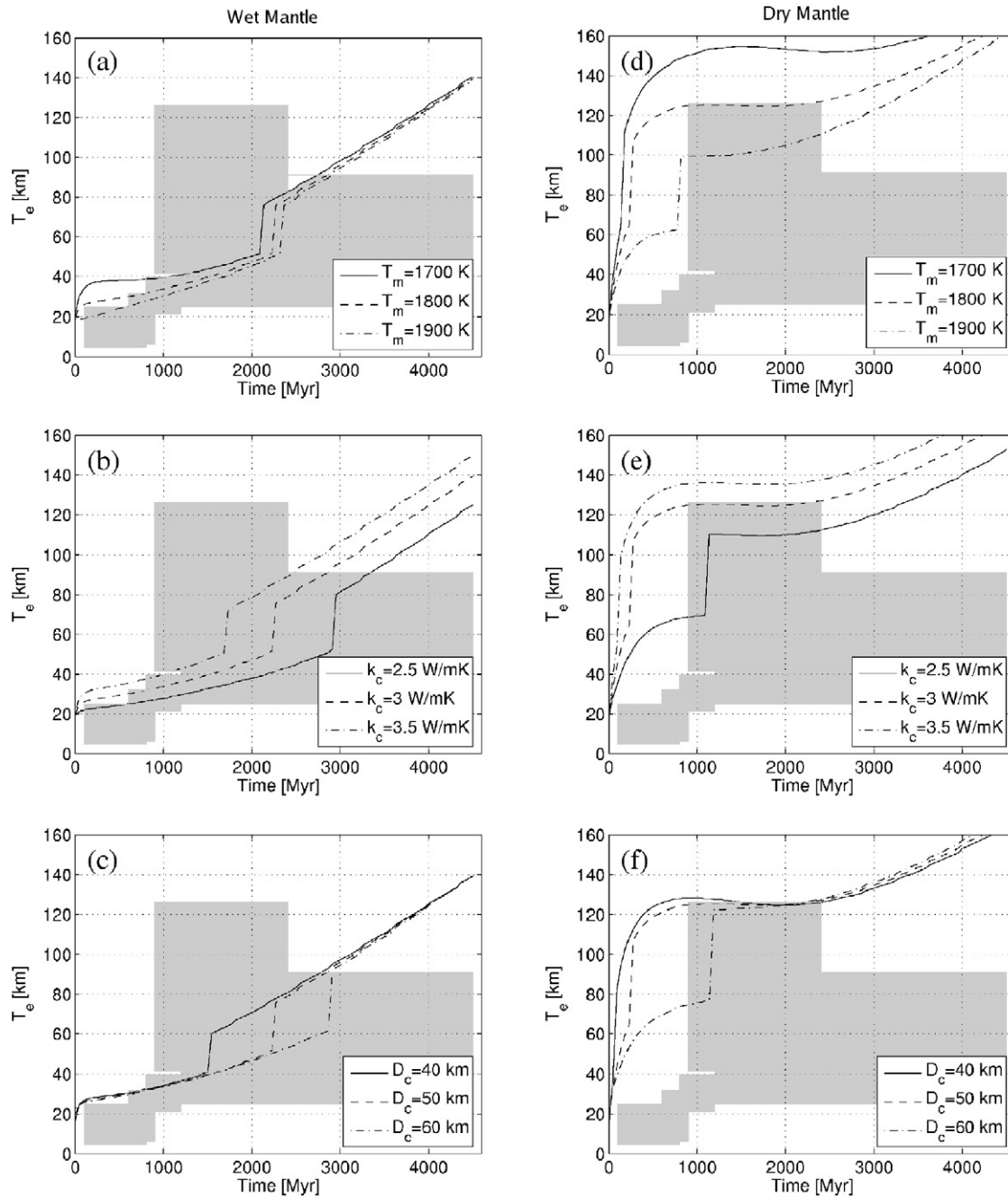


Fig. 4. The elastic thickness  $T_e$  as a function of time for thermal evolution models with a wet crustal rheology, varying initial upper mantle temperature  $T_m$ , crustal thermal conductivity  $k_c$  and crustal thickness  $D_c$ . (a–c) Wet mantle rheology and  $\eta_0 = 10^{19}$  Pa s, (d–f) dry mantle rheology and  $\eta_0 = 10^{21}$  Pa s. The mean elastic thicknesses given in Fig. 1b are indicated by shaded rectangles.

the lithosphere acts as a single plate during the entire evolution.

#### 4.2. Elastic thickness evolution

We have investigated the influence of crustal and mantle rheology on the evolution of the lithospheric thickness calculating the thermal evolution of the entire planet. Given the thermal structure of the lithosphere, elastic thickness values are derived from the corresponding strength envelopes and the results of the

calculations are shown in Figs. 4 and 5 for a wet and dry crustal rheology, respectively.

Figs. 4a–4c show the elastic thickness  $T_e$  as a function of time for thermal evolution models with a wet crustal and wet mantle rheology, varying initial upper mantle temperature  $T_m$ , crustal thermal conductivity  $k_c$  and crustal thickness  $D_c$ . The parameter ranges corresponding to the observed mean elastic thickness values (cf. Fig. 1) are indicated by shaded rectangles. Early in the evolution, the elastic thickness is small and varies between 20 and 40 km. Mechanical strength is carried by competent crustal and mantle layers which are separated by a layer

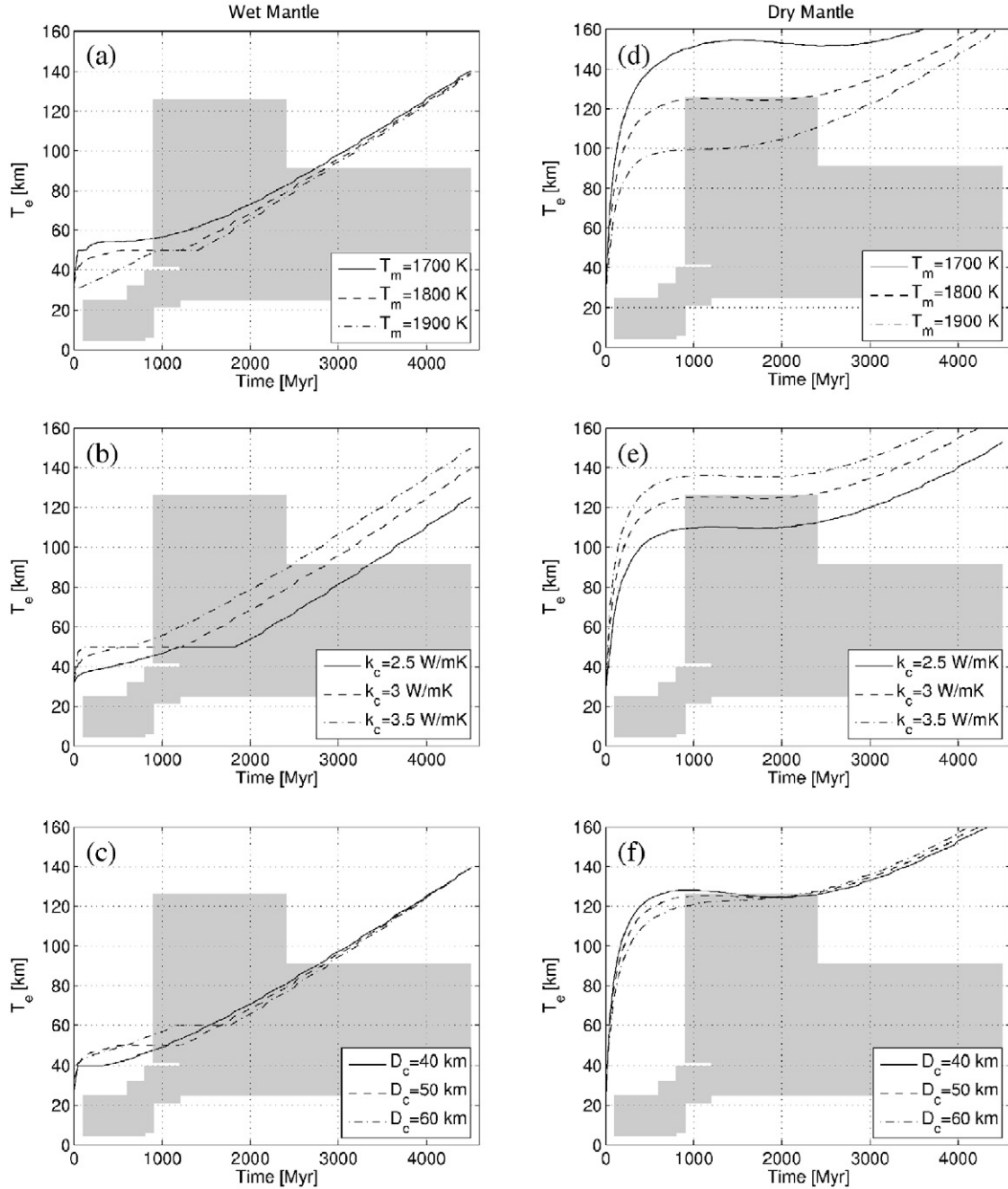


Fig. 5. Same as Fig. 4, but for thermal evolution models with a dry crustal rheology. (a–c) Wet mantle rheology and  $\eta_0 = 10^{19}$  Pa s, (d–f) dry mantle rheology and  $\eta_0 = 10^{21}$  Pa s.

of incompetent crust. Between 1.5 and 3 Gyr, elastic thickness values increase by  $\sim 30$  km, as the incompetent layer vanishes due to crustal cooling and the lithosphere acts as a single plate. Subsequent cooling then leads to a further continuous increase of  $T_e$ , with maximum values today around 140 km.

An increase of the initial upper mantle temperature (Fig. 4a) results in a warmer lithosphere and elastic thickness is therefore reduced. Furthermore, the rapid increase of elastic thickness due to the coupling of competent crustal and mantle layers occurs later. If thermal conductivity is increased (Fig. 4b), the insulating effect of the crust is reduced and the lithosphere cools more efficiently. This results in larger elastic thicknesses and

layer coupling is shifted to earlier times. An increase of the thermal conductivity therefore has a similar effect as a reduction of the crustal thickness (Fig. 4c), i.e., the insulation is reduced. For low  $D_c$ , elastic thickness is larger and the layer coupling occurs earlier in the evolution. This general dependence of the  $T_e$  on  $T_m$ ,  $k_c$  and  $D_c$  holds for all rheologies considered.

Figs. 4d–4f are similar to Figs. 4a–4c, but for a dry mantle rheology. Elastic thickness is large already early in the evolution, with  $T_e$  larger than 60 km already before 1 Gyr. This is partly due to the large mantle contribution to the total strength, but also owes to the low lithospheric temperatures as a consequence of the inefficient mantle convection and the thick

thermal boundary layers. Welding of the crustal and mantle sublayers occurs early in the evolution, usually before 1 Gyr. After the loss of the incompetent crustal layer, elastic thickness grows slowly, reflecting the slow cooling of the planet, and elastic thickness values in excess of 160 km are reached today.

The results for a dry crustal rheology are summarized in Fig. 5. If the mantle is assumed to be wet (Figs. 5a–5c), elastic thickness grows continuously from values around 40 km at 0.5 Gyr to ~140 km today. During the early evolution strength is carried by the crust alone and the mantle starts to contribute only after it has sufficiently cooled. No incompetent crustal layer above the competent mantle develops and thus no rapid increase of the lithospheric thickness is observed.

If both crust and mantle are assumed to be dry (Figs. 5d–5f), lithospheric strength is large essentially during the entire evolution. A dry mantle results in a cool lithosphere and the strong rheologies then yield elastic thickness values in excess of 100 km already after 500 Myr. No incompetent crustal layer is present and lithospheric thickness grows continuously after an initial cooling phase and reaches values in excess of 160 km today. Due to the inefficient mantle convection connected to the stiff mantle rheology, cooling and lithospheric growth are small after 500 Myr.

## 5. Discussion

The elastic thickness data compiled in Fig. 1b show low  $T_e$  around 20 km in the Noachian to Hesperian periods and large  $T_e$  around 70 km during the Hesperian to Amazonian periods, with a phase of rapid lithospheric thickening in the Hesperian. These observations are best compatible with a wet crustal and wet mantle rheology, as this combination yields low elastic thicknesses during the early evolution. Furthermore, the rapid increase of lithospheric strength in the Hesperian is explained in terms of the vanishing of the incompetent crustal layer at that time. Note, that the exact timing of lithospheric growth and layer coupling are model dependent and should not be used to constrain crustal and mantle rheologies. Apart from the isolating influence of the low conductivity crustal layer (cf. Figs. 4b–4c), other parameters such as the bounding stress  $\sigma_y$  affect the time at which the incompetent crustal layer vanishes. Furthermore, the timing is also sensitive to the rate of planetary cooling and thus depends on the activation energy  $A$  for viscous deformation, with smaller  $A$  resulting in efficient cooling and earlier layer coupling.

Although the rapid growth of the elastic thickness is also predicted for a wet crustal and dry mantle rheology (Figs. 4d–4f), the increase occurs very early in the evolution. Furthermore,  $T_e$  is rather large early on, contrary to observations. However, the exact time of the rapid  $T_e$  increase does not serve as a hard constraint (see above). Also, we have so far assumed that no bending stresses are acting on the lithospheric plate and flexure due to loading can reduce  $T_e$  by brittle and ductile yielding (McNutt, 1984). Depending on the curvature, elastic thicknesses may be reduced by up to a factor of two, making it easier to reconcile the dry mantle results with the observa-

tions. Therefore, a dry mantle rheology cannot be ruled out at present. However, if the martian mantle were dry, high initial upper mantle temperatures and a strongly thermally isolating crust would be required to yield the observed low elastic thickness values during the Noachian.

Finally, if a dry martian crust is considered, the rapid increase of  $T_e$  during the Hesperian is missing. As this increase is considered to be a diagnostic feature of the elastic thickness evolution, a dry basaltic rheology for the martian crust can be ruled out.

The results presented here are insensitive to the bulk abundance of heat-producing elements and their distribution between crust and mantle. If the abundance of radioactive species is larger (e.g., Lodders and Fegley, 1997), mantle and lithosphere will be warmer than assumed here. However, this will only affect the time of layer coupling and not change our main conclusions. Similarly, if more heat-producing elements were concentrated in the crust (Taylor et al., 2006), lithospheric cooling would be hampered, resulting in smaller  $T_e$  and later layer coupling.

The strain rate assumed here depends on the active deformation mechanism and may vary substantially for different settings. Larger  $\dot{\epsilon}$  yields stiffer behavior, larger  $T_e$  and the coupling between crust and mantle will occur earlier. However, the influence of the strain rate on the results is small and an increase of  $\dot{\epsilon}$  by one order of magnitude increases  $T_e$  by only 3 km, shifting the time of layer coupling by 300 Myr.

A necessary and sufficient condition for the rapid  $T_e$  growth to occur is the presence of a low yield temperature crust in combination with a high yield temperature mantle rheology. For the rheologies investigated here, this condition is satisfied if a wet crust is combined with a wet or dry mantle, resulting in yield temperature differences of 180 and 320 K, respectively. Therefore, the results presented here are equally applicable to, e.g., plagioclase rheologies (Rybacki and Dresen, 2000), although geochemical evidence suggests that the bulk of the martian crust is basaltic (Nimmo and Tanaka, 2005).

Note, however, that predictions of the water content of the crust are only possible if the stiffness of the dry candidate crustal material is comparable to that of the mantle. Dry granite, for example, would be considerably weaker than mantle material (Hansen and Carter, 1983; Watts, 2001) and an incompetent crustal layer would be present during the early evolution. Therefore, the rapid increase of  $T_e$  connected to the vanishing of this layer can occur even for dry crustal rheologies, provided that they are weak enough.

It has been suggested that the martian crust might have been hydrothermally cooled during the early planetary evolution (Parmentier and Zuber, 2007). To estimate the influence of a hydrothermally cooled crust, we have calculated the elastic thickness evolution for a model including a 20 km thick brecciated and hydrothermally cooled crustal layer. Using the approach by Parmentier and Zuber (2007) and assuming a Nusselt number of 2, a small increase of  $T_e$  by 4 km and a shift of the layer coupling to earlier times by ~200 is observed. Hydrothermal cooling of the crust therefore only has a small in-

fluence on the elastic thickness evolution and is consistent with the results presented here.

## 6. Conclusions

Elastic thickness data indicate that the martian elastic lithosphere was initially relatively thin and increased its thickness rapidly during the Hesperian period. We have modeled the thermal evolution of Mars and studied the influence of crustal and mantle rheology on the evolution of the lithospheric thickness and found that the observations are best compatible with a wet crust and wet mantle rheology. A dry mantle rheology cannot be ruled out at present but generally yields too large  $T_e$  early in the evolution. A dry basaltic rheology of the martian crust is incompatible with the observations as these models cannot explain the rapid lithospheric growth during the Hesperian.

The rapid growth of the elastic lithosphere thickness in the Hesperian was found to be a consequence of the lithosphere's multilayer rheology. While a layer of incompetent crust separates the mechanically strong crustal and mantle layers during the early evolution, planetary cooling causes this layer to vanish later on. The resulting single plate is mechanically much stronger than the two unwelded components and large elastic thicknesses are obtained, similar to what is observed on Earth's continents (Burov and Diament, 1995).

Mars exhibits a bimodal crustal thickness distribution, with peaks around 32 and 58 km (Neumann et al., 2004). Although a laterally varying crustal thickness cannot be self-consistently integrated into the one-dimensional models presented here, a first order estimate of the influence of the crustal dichotomy may be obtained by comparing the results for the different crustal thicknesses appropriate for the two provinces. For wet rheologies and  $D_c = 30$  km, coupling between crust and mantle occurs as early as 500 Myr after core formation, whereas for  $D_c = 60$  km the incompetent crustal layer only vanishes after 2800 Myr. It therefore seems likely that crust and mantle were mechanically decoupled when the Hesperian aged wrinkle ridges formed in the southern highlands, whereas the incompetent crustal layer had probably already vanished in the northern lowlands at that time. This has in fact been suggested as the cause for the different spacing of Hesperian aged wrinkle ridges in these two provinces (Montési and Zuber, 2003) and provides further support for the analysis presented here.

A phase of magma-ocean overturn during the early martian evolution would have resulted in a stable mantle stratification (Elkins-Tanton et al., 2003), suppressing thermal convection. The planet would have therefore cooled by heat conduction alone, yielding a massive stagnant lid and extremely low lithospheric temperatures. If convection did not initiate within a few hundred Myrs, the resulting elastic thicknesses must therefore be expected to be very large. Therefore, models including magma-ocean overturn are difficult to reconcile with the low observed  $T_e$  during the Noachian period.

The presented results are consistent with an early, deep seated global scale hydrological system on Mars (Parmentier and Zuber, 2007; Andrews-Hanna et al., 2007), which would

be conducive to a wet crustal rheology. A wet crust could provide the pore fluid necessary for hydrothermal cooling of the crust, thus preventing viscous relaxation of topography during the early martian evolution (Parmentier and Zuber, 2007). Furthermore, faults on Mars have been shown to be relatively weak (Barnett and Nimmo, 2002; Grott et al., 2005) compared to faults on Venus (Foster and Nimmo, 1996) and Mercury (Nimmo, 2002) and this weakness has been interpreted as the effect of pore fluid pressure, a conjecture consistent with the results presented here.

## Acknowledgments

We wish to thank J.C. Andrews-Hanna and an anonymous reviewer for careful and constructive reviews, which helped to improve this manuscript.

## References

- Andrews-Hanna, J.C., Phillips, R.J., Zuber, M.T., 2007. Meridiani Planum and the global hydrology of Mars. *Nature* 446, 163–165.
- Barnett, D.N., Nimmo, F., 2002. Strength of faults on Mars from MOLA topography. *Icarus* 157, 34–42.
- Belleguic, V., Lognonne, P., Wieczorek, M., 2005. Constraints on the martian lithosphere from gravity and topography data. *J. Geophys. Res.* 110, doi:10.1029/2005JE002437. E11005.
- Breuer, D., Spohn, T., 2003. Early plate tectonics versus single-plate tectonics on Mars: Evidence from magnetic field history and crust evolution. *J. Geophys. Res.* 108 (E7), doi:10.1029/2002JE001999. 5072.
- Burov, E.B., Diament, M., 1995. The effective elastic thickness ( $T_e$ ) of continental lithosphere: What does it really mean? *J. Geophys. Res.* 100 (B3), 3905–3927.
- Byerlee, J.D., 1978. Friction of rocks. *Pure Appl. Geophys.* 116, 615–626.
- Caldwell, J.G., Turcotte, D.L., 1979. Dependence of the thickness of the elastic oceanic lithosphere on age. *J. Geophys. Res.* 84 (B13), 7572–7576.
- Caristan, Y., 1982. The transition from high temperature creep to fracture in Maryland diabase. *J. Geophys. Res.* 87, 6781–6790.
- Choblet, G., Sotin, C., 2000. 3D thermal convection with variable viscosity: Can transient cooling be described by a quasi-static scaling law? *Phys. Earth Planet. Inter.* 119 (3–4), 321–336.
- Clauser, C., Huenges, E., 1995. Thermal conductivity of rocks and minerals. In: Ahrens, T.J. (Ed.), *Rock Physics and Phase Relations: A Handbook of Physical Constants*. In: AGU Ref. Shelf, vol. 3. AGU, Washington, DC, pp. 105–126.
- Cochran, J.R., 1980. Some remarks on isostasy and the long-term behavior of the continental lithosphere. *Earth Planet. Sci. Lett.* 46 (2), 266–274.
- Connerney, J.E.P., Acuña, M.H., Ness, N.F., Kletetschka, G., Mitchell, D.L., Lin, R.P., Reme, H., 2005. Tectonic implications of Mars crustal magnetism. *Proc. Natl. Acad. Sci. USA* 102 (42), 14970–14975.
- Davaille, A., Jaupart, C., 1993. Transient high Rayleigh number thermal convection with large viscosity variations. *J. Fluid Mech.* 253, 141–166.
- Dreibus, G., Wanke, H., 1987. Volatiles on Earth and Mars—A comparison. *Icarus* 71, 225–240.
- Elkins-Tanton, L.T., Parmentier, E.M., Hess, P.C., 2003. Magma ocean fractional crystallization and cumulate overturn in terrestrial planets: Implications for Mars. *Meteorit. Planet. Sci.* 38 (12), 1753–1771.
- Elkins-Tanton, L.T., Zaranek, S.E., Parmentier, E.M., Hess, P.C., 2005. Early magnetic field and magmatic activity on Mars from magma ocean cumulate overturn. *Earth Planet. Sci. Lett.* 236 (1–2), 1–12.
- Foster, A., Nimmo, F., 1996. Comparisons between the rift systems of East Africa, Earth and Beta Regio, Venus. *Earth Planet. Sci. Lett.* 143, 183–195.
- Grasset, O., Parmentier, E.M., 1998. Thermal convection in a volumetrically heated, infinite Prandtl number fluid with strongly temperature-dependent viscosity: Implications for planetary evolution. *J. Geophys. Res.* 103, 18171–18181.

- Grott, M., 2005. Late crustal growth on Mars: Evidence from lithospheric extension. *Geophys. Res. Lett.* 32, doi:10.1029/2005GL024492. L23201.
- Grott, M., Hauber, E., Werner, S.C., Kronberg, P., Neukum, G., 2005. High heat flux on ancient Mars: Evidence from rift flank uplift at Coracis Fossae. *Geophys. Res. Lett.* 32, doi:10.1029/2005GL023894. L21201.
- Grott, M., Hauber, E., Werner, S.C., Kronberg, P., Neukum, G., 2007. Mechanical modeling of thrust faults in the Thaumasia region, Mars, and implications for the Noachian heat flux. *Icarus* 186, 517–526.
- Hansen, F.D., Carter, N.L., 1983. Semibrittle creep of dry and wet Westerly granite at 1000 MPa. In: 24th US Symposium on Rock Mechanics, Texas A&M University, College Station, pp. 429–447.
- Hartmann, W.K., Berman, D.C., 2000. Elysium Planitia lava flows: Crater count chronology and geological implications. *J. Geophys. Res.* 105 (E6), doi:10.1029/1999JE001189, 15011–15026.
- Hartmann, W.K., Neukum, G., 2001. Cratering chronology and the evolution of Mars. *Space Sci. Rev.* 96, 165–194.
- Hartmann, W.K., Malin, M., McEwen, A., Carr, M., Soderblom, L., Thomas, P., Danielson, E., James, P., Veverka, J., 1999. Evidence for recent volcanism on Mars from crater counts. *Nature* 397 (6720), 586–589.
- Hauck, S.A., Phillips, R.J., 2002. Thermal and crustal evolution of Mars. *J. Geophys. Res.* 107 (E7), doi:10.1029/2001JE001801. 5052.
- Karato, S.-I., Wu, P., 1993. Rheology of the upper mantle: A synthesis. *Science* 260, 771–778.
- Karato, S.-I., Paterson, M.S., Fitzgerald, J.D., 1986. Rheology of synthetic olivine aggregates—Influence of grain size and water. *J. Geophys. Res.* 91, 8151–8176.
- Karner, G.D., Steckler, M.S., Thorne, J.A., 1983. Long-term thermo-mechanical properties of the continental lithosphere. *Nature* 304, 250–253.
- Kronberg, P., Hauber, E., Grott, M., Werner, S.C., Schäfer, T., Gwinner, K., Giese, B., Masson, P., Neukum, G., 2007. Acheron Fossae, Mars: Tectonic rifting, volcanism, and implications for lithospheric thickness. *J. Geophys. Res.* 112, doi:10.1029/2006JE002780. E04005.
- Kruse, S.E., Royden, L.H., 1994. Bending and unbending of an elastic lithosphere: The Cenozoic history of the Apennine and Dinaride foredeep basins. *Tectonics* 13 (2), 278–302.
- Lodders, K., Fegley, B., 1997. An oxygen isotope model for the composition of Mars. *Icarus* 126 (2), 373–394.
- Mackwell, S.J., Zimmerman, M.E., Kohlstedt, D.L., 1998. High-temperature deformation of dry diabase with application to tectonics on Venus. *J. Geophys. Res.* 103 (B1), 975–984.
- McGovern, P.J., Solomon, S.C., Smith, D.E., Zuber, M.T., Simons, M., Wicczorek, M.A., Phillips, R.J., Neumann, G.A., Aharonson, O., Head, J.W., 2004. Correction to “Localized gravity/topography admittance and correlation spectra on Mars: Implications for regional and global evolution”. *J. Geophys. Res.* 109, doi:10.1029/2004JE002286. E07007.
- McNutt, M., 1984. Lithospheric flexure and thermal anomalies. *J. Geophys. Res.* 89, 11180–11194.
- McNutt, M., 1990. Flexure reveals great depth. *Nature* 343, 596–597.
- McNutt, M., Menard, H.W., 1982. Constrains on the yield strength in the oceanic lithosphere derived from observations of flexure. *Geophys. J. R. Astron. Soc.* 59, 4663–4678.
- McNutt, M.K., Diament, M., Kogan, M.G., 1988. Variations of elastic plate thickness at continental thrust belts. *J. Geophys. Res.* 93, 8825–8838.
- McSween, H.Y., Grove, T.L., Lentz, R.C.F., Dann, J.C., Holzheid, A.H., Ricuputi, L.R., Ryan, J.G., 2001. Geochemical evidence for magmatic water within Mars from pyroxenes in the Shergotty meteorite. *Nature* 409, 487–490.
- Mei, S., Kohlstedt, D.L., 2000a. Influence of water on plastic deformation of olivine aggregates. 2. Dislocation creep regime. *J. Geophys. Res.* 105 (B9), doi:10.1029/2000JB900180, 21471–21482.
- Mei, S., Kohlstedt, D.L., 2000b. Influence of water on plastic deformation of olivine aggregates. 1. Diffusion creep regime. *J. Geophys. Res.* 105 (B9), doi:10.1029/2000JB900179, 21457–21470.
- Médard, E., Grove, T.L., 2006. Early hydrous melting and degassing of the martian interior. *J. Geophys. Res.* 111 (E11), doi:10.1029/2006JE002742. E11003.
- Mellon, M.T., Feldman, W.C., Prettyman, T.H., 2004. The presence and stability of ground ice in the southern hemisphere of Mars. *Icarus* 169 (2), 324–340.
- Montési, L.G.J., Zuber, M.T., 2003. Clues to the lithospheric structure of Mars from wrinkle ridge sets and localization instability. *J. Geophys. Res.* 108 (E6), doi:10.1029/2002JE001974. 2–1.
- Mueller, S., Phillips, R.J., 1995. On the reliability of lithospheric constraints derived from models of outer-rise flexure. *Geophys. J. Int.* 123, 887–902.
- Neukum, G., Jaumann, R., Hoffmann, H., Hauber, E., Head, J.W., Basilevsky, A.T., Ivanov, B.A., Werner, S.C., van Gasselt, S., Murray, J.B., McCord, T., and the HRSC Co-Investigator Team, 2004. Recent and episodic volcanic and glacial activity on Mars revealed by the High Resolution Stereo Camera. *Nature* 432 (7020), 971–979.
- Neumann, G.A., Zuber, M.T., Wicczorek, M.A., McGovern, P.J., Lemoine, F.G., Smith, D.E., 2004. Crustal structure of Mars from gravity and topography. *J. Geophys. Res.* 109, doi:10.1029/2004JE002262. E08002.
- Nimmo, F., 2002. Constraining the crustal thickness on Mercury from viscous topographic relaxation. *Geophys. Res. Lett.* 29 (5), doi:10.1029/2001GL013883. 1063.
- Nimmo, F., Stevenson, D.J., 2000. Influence of early plate tectonics on the thermal evolution and magnetic field of Mars. *J. Geophys. Res.* 105 (E5), doi:10.1029/1999JE001216, 11969–11979.
- Nimmo, F., Stevenson, D.J., 2001. Estimates of martian crustal thickness from viscous relaxation of topography. *J. Geophys. Res.* 106, 5085–5098.
- Nimmo, F., Tanaka, K., 2005. Early crustal evolution of Mars. *Annu. Rev. Earth Planet. Sci.* 33, 133–161.
- Parmentier, E.M., Zuber, M.T., 2007. Early evolution of Mars with mantle compositional stratification or hydrothermal crustal cooling. *J. Geophys. Res.* 112, doi:10.1029/2005JE002626. E02007.
- Richter, F.M., 1978. Mantle convection models. *Annu. Rev. Earth Planet. Sci.* 6, 9–19.
- Rybacki, E., Dresen, G., 2000. Dislocation and diffusion creep of synthetic anorthite aggregates. *J. Geophys. Res.* 105 (B11), doi:10.1029/2000JB900223, 26017–26036.
- Sahagian, D.L., Holland, S.M., 1993. On the thermo-mechanical evolution of continental lithosphere. *J. Geophys. Res.* 98 (B5), 8261–8274.
- Schubert, G., Spohn, T., 1990. Thermal history of Mars and the sulfur content of its core. *J. Geophys. Res.* 95, 14095–14104.
- Schubert, G., Cassen, P., Young, R.E., 1979. Subsidiary convective cooling histories of terrestrial planets. *Icarus* 38, 192–211.
- Schultz, R.A., Watters, T.R., 2001. Forward mechanical modeling of the Amathes Rupes thrust fault on Mars. *Geophys. Res. Lett.* 28, 4659–4662.
- Schumacher, S., Breuer, D., 2006. Influence of a variable thermal conductivity on the thermochemical evolution of Mars. *J. Geophys. Res.* 111 (E2), doi:10.1029/2005JE002429. E02006.
- Seipold, U., 1998. Temperature dependence of thermal transport properties of crystalline rocks—A general law. *Tectonophysics* 291, 161–171.
- Spohn, T., 1991. Mantle differentiation and thermal evolution of Mars, Mercury, and Venus. *Icarus* 90, 222–236.
- Spohn, T., Schubert, G., 1982. Modes of mantle convection and the removal of heat from the Earth’s interior. *J. Geophys. Res.* 87, 4682–4696.
- Taylor, G.J., Boynton, W., Brückner, J., Wänke, H., Dreibus, G., Kerry, K., Keller, J., Reedy, R., Evans, L., Starr, R., Squyres, S., Karunatillake, S., Gasnault, O., Maurice, S., d’Uston, C., Englert, P., Dohm, J., Baker, V., Hamara, D., Janes, D., Sprague, A., Kim, K., Drake, D., 2006. Bulk composition and early differentiation of Mars. *J. Geophys. Res.* 111 (E3), doi:10.1029/2005JE002645. E03S10.
- Treiman, A.H., Drake, M.J., Janssens, M.-J., Wolf, R., Ebihara, M., 1986. Core formation in the Earth and shergottite parent body (SPB)—Chemical evidence from basalts. *Geochim. Cosmochim. Acta* 50, 1071–1091.
- Turcotte, D.L., Schubert, G., 2002. *Geodynamics*, second ed. Cambridge Univ. Press, New York. 456 pp.
- Watts, A.B., 1978. An analysis of isostasy in the world’s oceans. 1. Hawaiian-emperor seamount chain. *J. Geophys. Res.* 83 (B12), 5989–6004.
- Watts, A.B., 1992. The effective elastic thickness of the lithosphere and the evolution of foreland basins. *Basin Res.* 4, 169–178.
- Watts, A.B., 2001. *Isostasy and Flexure of the Lithosphere*. Cambridge Univ. Press, Cambridge, UK.

- Watts, A.B., Burov, E.B., 2003. Lithospheric strength and its relationship to the elastic and seismogenic layer thickness. *Earth Planet. Sci. Lett.* 213 (1–2), 113–131.
- Watts, A.B., Bodine, J.H., Ribe, N.M., 1980. Observations of flexure and the geological evolution of the Pacific Ocean basin. *Nature* 283, 532–537.
- Wieczorek, M.A., Zuber, M.T., 2004. Thickness of the martian crust: Improved constraints from geoid-to-topography ratios. *J. Geophys. Res.* 109 (E1), doi:10.1029/2003JE002153. E01009.
- Williams, J.-P., Nimmo, F., 2004. Thermal evolution of the martian core: Implications for an early dynamo. *Geology* 32, 97–100.
- Zuber, M.T., Solomon, S.C., Phillips, R.J., Smith, D.E., Tyler, G.L., Aharonson, O., Balmino, G., Banerdt, W.B., Head, J.W., Johnson, C.L., Lemoine, F.G., McGovern, P.J., Neumann, G.A., Rowlands, D.D., Zhong, S., 2000. Internal structure and early thermal evolution of Mars from Mars Global Surveyor topography and gravity. *Science* 287, 1788–1797.